Thin–Walled Structures 123 (2018) 520–527

Contents lists available at ScienceDirect

Thin–Walled Structures

journal homepage: www.elsevier.com/locate/tws

A component method for cold-formed steel beam-to-column bolted gusset plate joints

Žilvinas Bučmys[a,*], Alfonsas Daniūnas[a], Jean-Pierre Jaspart[b], Jean-Francois Demonceau[b]

[a] Dept. of Steel And Timber Structures, Faculty of Civil Engineering, Vilnius Gediminas Technical University, Saulėtekio al. 11, 10223 Vilnius, Lithuania
[b] Dept. ArGEnCo, Liege University, Allée de la Découverte 9, 4000 Liege, Belgium

ARTICLE INFO

Keywords:
Semi-rigid joints
Component method
Cold-formed steel joints

ABSTRACT

Cold-formed steel elements are being used more frequently on construction sites because of the good strength-to-cost ratio. Researches on such structures show that, in most cases, the behaviour of the constitutive joints is semi-rigid. However, insufficient studies are published examining the properties of these joints. This paper presents a study of cold-formed steel bolted gusset plate connections based on the component method approach. The component method considers any joint as a set of individual basic components. In this procedure, the joints are analysed using mechanical models that are able to simulate moment – rotation $M - \varphi$ relationship. In this paper the joint is analysed as made of three springs: beam bolt group, column bolt group and gusset plate. A "three springs" mechanical model and a technique to calculate joint stiffness is presented. The results predicted through the proposed mechanical model are validated through comparisons to experimental and finite element results.

1. Introduction

Traditionally the joints in steel structures are characterised as rigid or pinned. In the last few decades, the concept of semi-rigid joints became more popular. Modern standards for steel design like Eurocode 3 allow one to take into account the actual joint behaviour, i. e. semi-rigid and / or partial strength joints. As a result economy may be reached in the design of the frame members. The researches on steel frames with semi-rigid joints showed that the stiffness of the joints has a significant influence on the behaviour of the frame response [1–5]. The account for the joints real behaviour allows designing safer structures and reaching an economical benefit [6–11].

In recent years, researches on thin-walled sections focused on the experimental investigation of beam-to-beam joints and beam elements [12]. Previous publications present the result of a wide variety of experimental tests and numerical simulations; however, most of them are not dealing with the evaluation of the joint stiffness. But investigators who performed laboratory tests especially on purlin over-lapped [13–18], sleeve [19–22] and apex [23–27] cold-formed joints and analysed data of joint strength and stiffness agreed that the behaviour of such joints is actually semi-rigid.

This statement, however, is only based on the results of experimental tests and numerical simulations performed on beam-to-column gusset plate bolted joints [28–33]. In addition, the researchers noted that bearing deformations around bolts have a significant impact on the flexibility of the joints. For daily practise, there is a lack of accurate analytical methods to predict the stiffness of these joints. And without such stiffness evaluation methods, the influence of the stiffness on the frame rresponse could not be determined (in terms of forces and deflections of the structure).

The goal of this paper is to present a "three springs" mechanical model to calculate the stiffness of cold-formed steel gusset plate bolted connections (Fig. 1). The mechanical model adapts Eurocode 3 formulations that originally are suitable for elements of 3 mm and thicker. It is shown to provide a good agreement with experimental tests and numerical simulations.

2. Mechanical model with rotational springs for stiffness calculation of a bolted gusset-plate joint

2.1. Component method

The general assumption of the component method [34–38] for steel joints is to decompose the joint into a limited number of basic components. The first step of the component method is to identify all components that are active in shear, compression and tension zones amongst those listed in Eurocode 3 Part 1–8 [39]. The next step is to determine their local design resistances $F_{i,Rd}$ and stiffness coefficients

* Corresponding author.
E-mail address: zilvinas.bucmys@vgtu.lt (Ž. Bučmys).

https://doi.org/10.1016/j.tws.2016.10.022
Received 30 April 2016; Received in revised form 24 October 2016; Accepted 27 October 2016
Available online 04 January 2018
0263-8231/

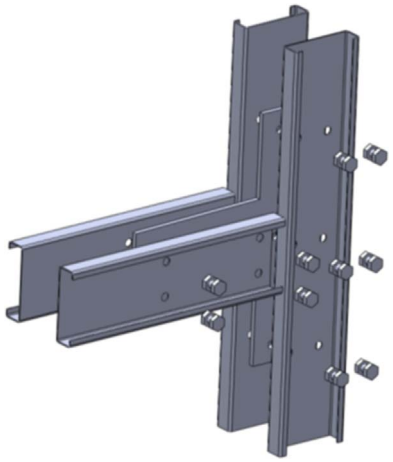

Fig. 1. The exploded view of the joint under analysis.

k_i before, at the last step, deriving the global joint properties: the design moment resistance $M_{j,Rd}$ and the initial stiffness $S_{j,ini}$, respectively. All necessary formulae describing the design resistances and the stiffness coefficients of the active components are provided in Eurocode 3 Part 1–8. The main disadvantage is that Eurocode 3 describes only a limited number of components met in the most commonly used joints. In fact, even if cold formed gusset plate joints are not explicitly addressed in Eurocode 3 Part 1–8, one realise quickly that all components active in these specific joints are covered by Eurocode 3 Part 1–8 rules; this is clearly the biggest interest of the component method proposed by Eurocode 3.

2.2. A "three springs" mechanical model

The mechanical model uses the component method and separates the joint into three separate rotational springs (Fig. 2): beam bolt group, column bolt group and gusset plate.

A load F applied to the beam generates, in addition to a shear force, a bending moment M_1 in the beam bolt group and a bending moment M_2 in the column bolt group. As a result, the bolt groups and the gusset plate should be investigated separately because the bolt groups are affected by different bending moments (Fig. 3): $M_1 = F{\cdot}l_1$ for beam bolt group and gusset plate; $M_2 = F{\cdot}l_2$ for column bolt group and gusset plate.

2.3. A mechanical model for bolt group rotational spring stiffness calculation

According to Eurocode 3 Part 1–8, the stiffness calculation of both the column and beam bolt groups may be based on the response of the following active components:

– section web in bearing (overall 2 sections in bolt group);

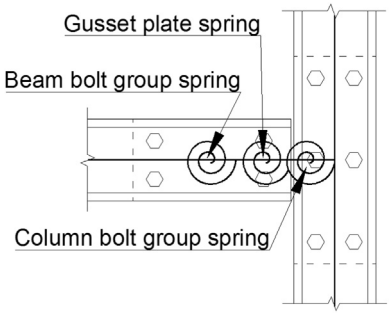

Fig. 2. A "three springs" mechanical model of the joint.

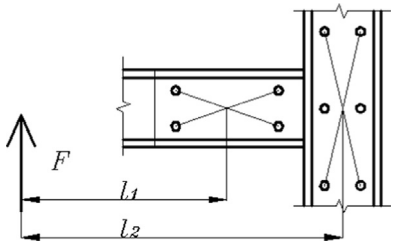

Fig. 3. Bending moments of three springs.

– gusset plate in bearing;
– bolts in shear (overall 2 shear planes in one bolt).

The stiffness of a single bolt can be expressed as sum of listed components, where values of k_{12a}, k_{12b} and k_{11} are presented in Eurocode 3 Part 1–8:

$$\frac{1}{k_b} = \sum \frac{1}{k_i} = \frac{1}{k_{12a}} + \frac{1}{k_{12b}} + \frac{1}{k_{11}} \tag{1}$$

where: k_b – the stiffness coefficient of a single bolt, k_i – the stiffness coefficient of the component i, k_{12a} – the stiffness coefficient of section web in bearing component, k_{12b} – the stiffness coefficient of gusset plate in bearing component, k_{11} – the stiffness coefficient of bolt in shear component.

Every single bolt in a bolt group is affected by force F_b that could be calculated from applied force F. The spring system for one bolt is depicted in Fig. 4a and the relationship of force F_b and deformation Δ_b is:

$$F_b = k_b E \Delta_b \tag{2}$$

where: k_b – the stiffness coefficient of a bolt, E – the Young modulus,

The mechanical model that allows integrating every single bolt extensional stiffness into a bolt group rotational stiffness is depicted in Fig. 4b. The stiffness of the bolt group can be expressed as:

$$S_{bg,ini} = \frac{M}{\varphi} = \frac{Ez_{b1}^2}{\frac{1}{k_{b1}}} + \ldots + \frac{Ez_{bn}^2}{\frac{1}{k_{bn}}} \tag{3}$$

where: M – bending moment, φ – rotation of joint, E – the Young modulus, z_{b1} , z_{bn} – distances between first and n pair of bolts (Fig. 4b), k_{b1} , k_{bn} – the stiffness coefficient of a single bolt.

2.4. A mechanical model for gusset plate rotational spring stiffness calculation

In Eurocode 3 Part 1–8, there is no suggestion for the stiffness calculation of a gusset plate. The rotation of the gusset plate φ has therefore been modelled as a sum of separate outstand element rotations φ_1, φ_2, φ_3 due to shear force V, bending moments M_1 and M (Fig. 5). As a result, in this paper, the stiffness of a gusset plate was calculated according to this formula:

$$S_{gp,ini} = \frac{M}{\varphi} = \frac{M}{\varphi_1 + \varphi_2 + \varphi_3} = \frac{M}{\frac{M_1 L_a}{EI_1} + \frac{VL_a^2}{2EI_1} + \frac{L_b^2 M}{2L_c EI_2}} = \frac{M}{\frac{2M_1 L_a + VL_a^2}{2EI_1} + \frac{L_b^2 M}{2L_c EI_2}} \tag{4}$$

where: L_a – distance from the rotation centre of the beam bolt group to the edge of gusset plate, L_b – distance from the outer bolt centre of the column bolt group to the edge of gusset plate, L_c – distance between outer bolts of the column bolt group, I_1 – the moment of inertia of the beam outstand element, I_2 – the moment of inertia of the column outstand element, V – shear force due to the beam load, M_1 and M bending moments of beam bolt group and column bolt group, respectively.

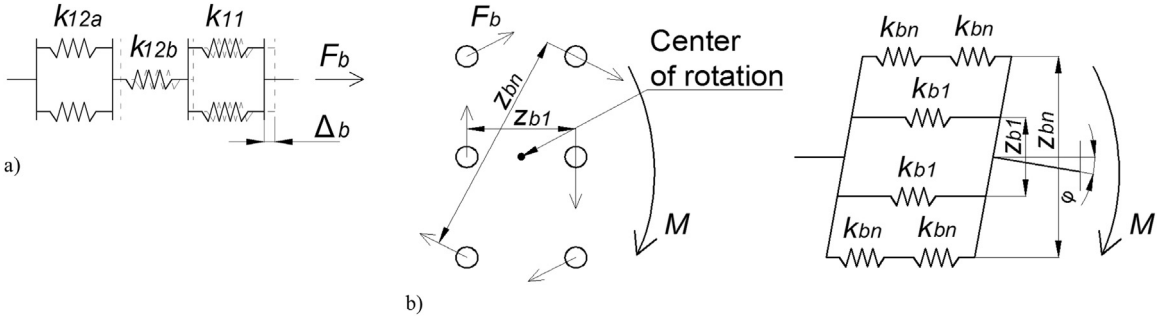

Fig. 4. (a) Extensional spring system for one bolt (b) Rotational spring for a bolt group.

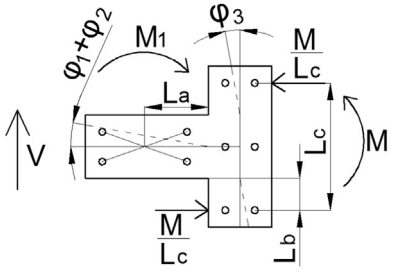

Fig. 5. The scheme for the rotation calculation of the gusset plate.

2.5. The rotational stiffness of joint

The rotation of joint is equal to the sum of the rotations obtained for the three springs (Fig. 6a):

$$\varphi_j = \varphi_{gp} + \varphi_{bbg} + \varphi_{cbg} \tag{5}$$

where: φ_j – the rotation of joint, φ_{gp} – the rotation of gusset plate, φ_{bbg} – the rotation of beam bolt group, φ_{cbg} – the rotation of column bolt group.

As a result the overall initial stiffness of the joint was calculated assembling the initial rotational stiffnesses of each spring using the formula below:

$$S_{j,ini} = \frac{1}{\frac{1}{S_{gp,ini}} + \frac{1}{S_{bbg,ini}} + \frac{1}{S_{cbg,ini}}} \tag{6}$$

where: $S_{gp,ini}$ – the initial stiffness of gusset plate, $S_{bbg,ini}$ – the initial stiffness of beam bolt group, $S_{cbg,ini}$ – the initial stiffness of column bolt group.

The $M - \varphi$ curve of springs and joints are depicted according to Eurocode 3 part 1–8 formulae (Fig. 6b). First slope of the graph corresponds to the linear behaviour which is valid provided that the bending moment M is less than 2/3 $M_{j,Rd}$ where $M_{j,Rd}$ is the moment resistance of the joint. The second slope is arc and the third slope is taken with a stiffness equal to zero. The third slope could be only be reached if failure mode is gusset plate due to bending moment or C-section web due to bearing. And otherwise in case then the failure mode are bolts in shear or local buckling of cold-formed sections the third slope could be neglected.

3. Experimental tests

3.1. Test specimen

Three specimens were investigated experimentally (Fig. 7). Gusset plates and cold-formed C-sections were made of steel grades S355 and S350GD+Z275 , respectively. The yield strength and the ultimate strength of both steel grades were measured by way of the coupon tests. As a result, the following values have been obtained for the cold-formed sections, f_y = 380 MPa and f_u = 484 MPa, and for the gusset plate, f_y = 442 MPa and f_u = 570 MPa, respectively. The specimens were connected using 8.8 bolts. The diameter of bolt holes was 1 mm higher than the bolt diameter. The spacing between bolts connecting the beam channel and the column channel to the gusset plate was 200 mm and 150 mm, respectively. The specimens differed by bolt diameter and C-section thickness:

- the first specimen (M12 C15015 T12) was made of 12 mm diameter bolts, 1.5 mm thick C-section and a 12 mm thick gusset plate;
- the second specimen (M12 C15025 T12) was made of 12 mm diameter bolts, 2.5 mm thick C-section and a 12 mm thick gusset plate;
- the third specimen (M16 C15015 T12) was made of 16 mm diameter bolts, 1.5 mm thick C-section and a 12 mm thick gusset plate.

The load was transferred by the jackscrew to the end of the beam. Pinned support was used at the top of the column and roller support at the bottom of the column. All the specimens were equipped with beam and column lateral restraints (Fig. 8a) so as to prevent lateral torsional buckling phenomena. A small part of the upper corner of beam was cut off so was no any contact with the column flange during rotational

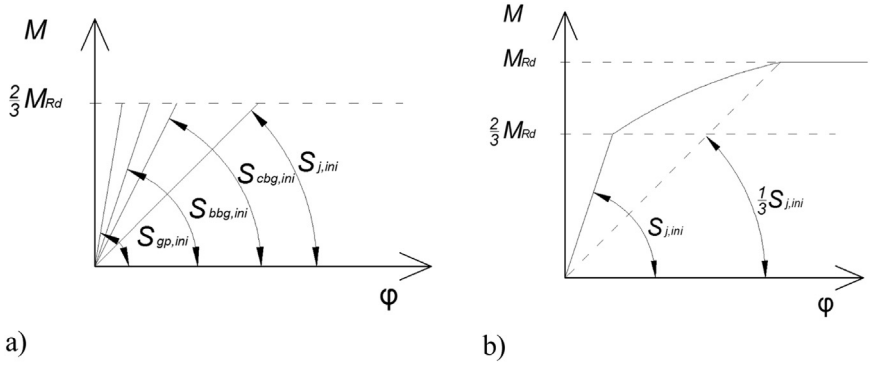

Fig. 6. (a) Initial rotational stiffness of springs and joint (b) $M - \varphi$ relationship of joint.

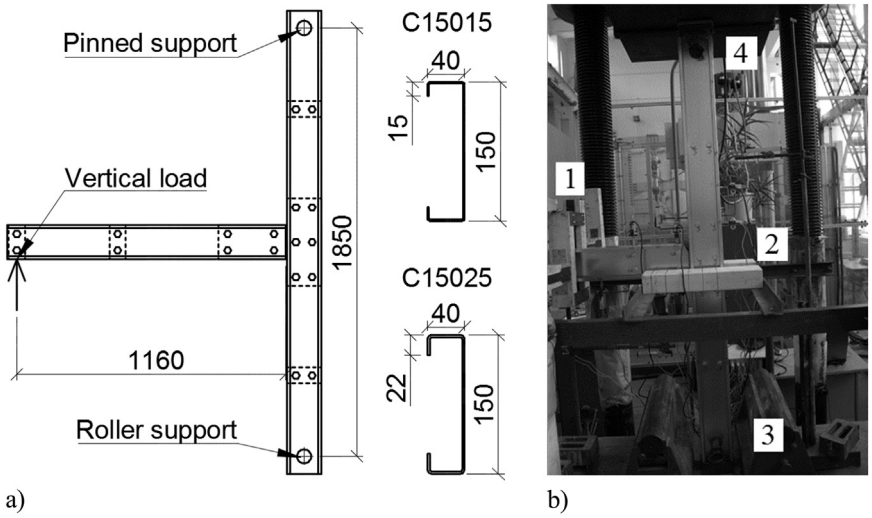

Fig. 7. (a) Geometrical properties of the specimens (b) 1, 2 – lateral restraints of the beam and the column, 3 – roller support with vertical moving direction, 4 – pinned support.

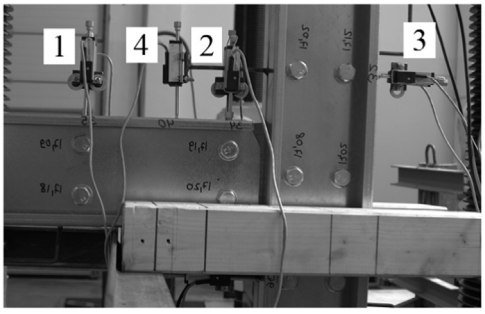

Fig. 8. Transducers for the measurement of rotations: 1,2 – beam bolt group; 3 – column bolt group; 4 – gusset plate.

deformations.

Transducers were added (Fig. 8b) to measure the rotation of the beam bolt group, column bolt group and gusset plate. Rotation due to slipping (which appear randomly depending on the initial position of the bolts in the holes) was eliminated for easier comparison with proposed mechanical models. The $M - \varphi$ curves including rotation due to slipping and the technique on how to convert transducers data measurements into rotation are described in Bučmys and Daniūnas paper [40].

3.2. Load capacity and failure modes of the specimens

The experimental failure load of the first specimen (M12 C15015 T12) was 10.22 kN and the failure mode was the local buckling in the beam (Fig. 9a). The experimental failure load of the second specimen (M12 C15025 T12) was 20.2 kN and the failure mode was the bolt collapse due to shear (Fig. 9b). The investigation after the test showed that bearing deformations around the holes of bolts and local buckling deformations in the beam had occurred. The failure load of the third test (M16 C15015 T12) was 10.7 kN with local buckling in the beam as failure mode (Fig. 9c).

4. Numerical simulations of the joints

4.1. Finite element type and material modelling

The numerical simulations were performed using Ansys Workbench software. The rotation and strength of the connection were investigated. The model was meshed using SOLID186 finite elements. SOLID186 is a higher order 3-D solid element that exhibits quadratic displacement behaviour. The element is defined by 20 nodes having three degrees of freedom per node: translations in the nodal x, y, and z directions. The element integrates plasticity and large deflections. Two layers of finite elements for cold formed sections and gusset plate were modelled.

Material non-linearity in the specimens was modelled with von Mises yield criterion and isotropic hardening (Fig. 10a). The stress-strain relationship of cold-formed steel profiles was described by a gradual yielding behaviour followed by a considerable period of strain hardening, whereas an elastic-plastic behaviour with strain hardening modulus less than 0,5% of elastic modulus E was assumed for the bolts and gusset plate. Stress – strain curves were taken from the coupon tests for cold formed steel sections and gusset plate. Bolts were modelled using characteristic material properties. The initial slope of cold-formed steel stress-strain curve was taken as the elastic modulus, E, of the material. Yielding of the steel was defined with 0,2% strain. Third slope was taken as less than 0,5% of elastic modulus E [41].

4.2. Loading, boundary, and contact conditions

The cross-sections, gusset plate and bolts, supports and loading were simulated according to laboratory tests using a three-dimensional numerical model (Fig. 10b). A concentrated force was applied at the end of the beam, as in the real tests. Pinned connection was modelled on the top of the column and roller support was modelled at the bottom of the column. To save time only half of the specimen was modelled using symmetry conditions. Finally, the translations in the perpendicular direction were constrained in order to prevent their lateral deformations. The contact between cold-formed profiles and gusset plate was modelled as frictional with a small friction coefficient. The contact between bolts and gusset plate was used rough and between bolts and cold-formed sections as frictionless. As in the laboratory tests the bolt hole diameter was modelled 1 mm higher than bolt one and to avoid rigid body motion a small bolt pretension of 100 N was applied. It is worth mentioning that rotation due to slipping was eliminated as in laboratory test results.

5. Results of component method, experimental and numerical calculations of the stiffness of the joints

In this chapter, $M - \varphi$ curves calculated using the component method, experimental tests and numerical simulations for the three springs and the joints are compared. Based on data from laboratory tests, experimental $M - \varphi$ curves were calculated using the technique described in Bučmys and Daniūnas 2015 paper. Stiffness using

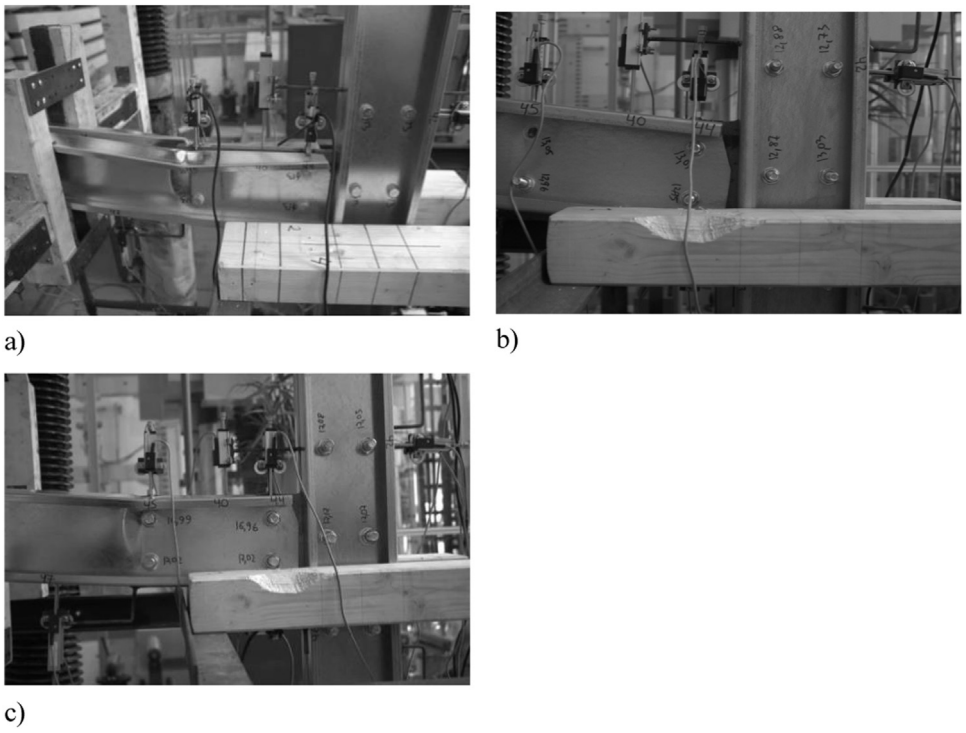

Fig. 9. Specimens at failure: (a) M12 C15015 T12; (b) M12 C15025 T12; (c) M16 C15015 T12.

component method was calculated according Part 1 of the paper. Bending capacity was calculated according Eurocode 3 rules. The joint was divided into the components: bolts in shear, section web in bearing, gusset plate in bearing, gusset plate in bending and shear, beam in bending and shear, column in bending and shear [40]. Then, taking into account the weakest component joint bending capacity $M_{j,Rd}$ was calculated. As mentioned in Part 2.1 of this paper, steel strength properties of the gusset plate and cold-formed sections for calculations using component method and numerical modelling were taken from coupon tests, and characteristic strength values (f_y = 640 MPa and f_u = 800 MPa, respectively) were used for the bolts.

$M - \varphi$ curves for the beam bolt group are presented in Fig. 11a, b, c and those for the column bolt group are presented in Fig. 12a, b, c. According to Eurocode 3 calculations, the failure load value of the specimen M12 C15015 T12 is 5% and 15% lower than those obtained experimentally and numerically, respectively. All the three investigations showed the same failure mode. Failure load value according to Eurocode 3 for the specimen M12 C15025 T12 is 3% and 11% lower compared with experimental test and numerical simulation, respectively. The failure mode according to both Eurocode 3 and numerical simulation was the same – local buckling in the beam that differed from experimental test. Failure load value according to Eurocode 3 calculations of the specimen M16 C15015 T12 is 10% and 16% lower compared with experimental test and numerical simulation, respectively, and the same failure mode. To sum up, the failure load value of the three specimens calculated according Eurocode 3 was up to 10% and 16% lower comparing with experimental results and numerical simulation, respectively. The stiffness calculated using component method showed a good agreement with experimental test and numerical simulation results.

$M - \varphi$ curves for the gusset plate are presented in Fig. 13a, b, c. Gusset plate stiffness calculated according to proposed formulae (4)

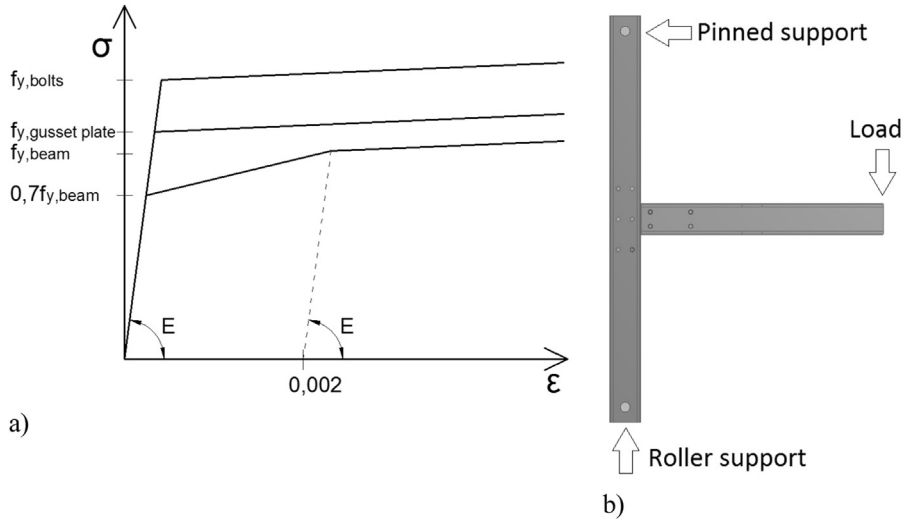

Fig. 10. (a) Stress – strain relationships; (b) Numerical model.

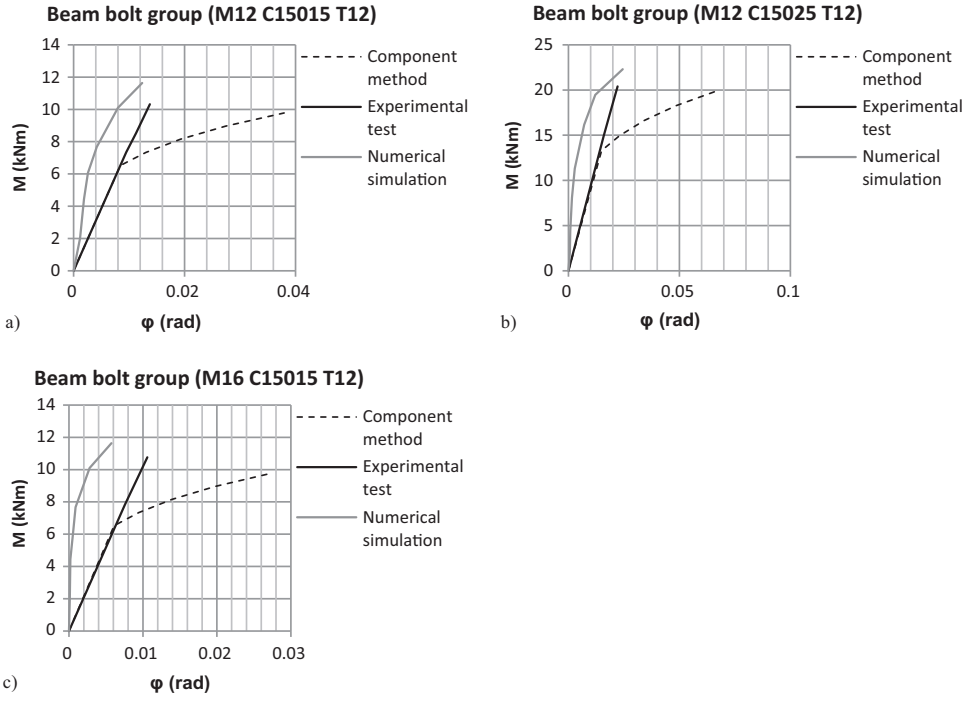

Fig. 11. $M - \varphi$ curves of the beam bolt group of the specimens: (a) M12 C15015 T12; (b) M12 C15025 T12; (c) M16 C15015 T12.

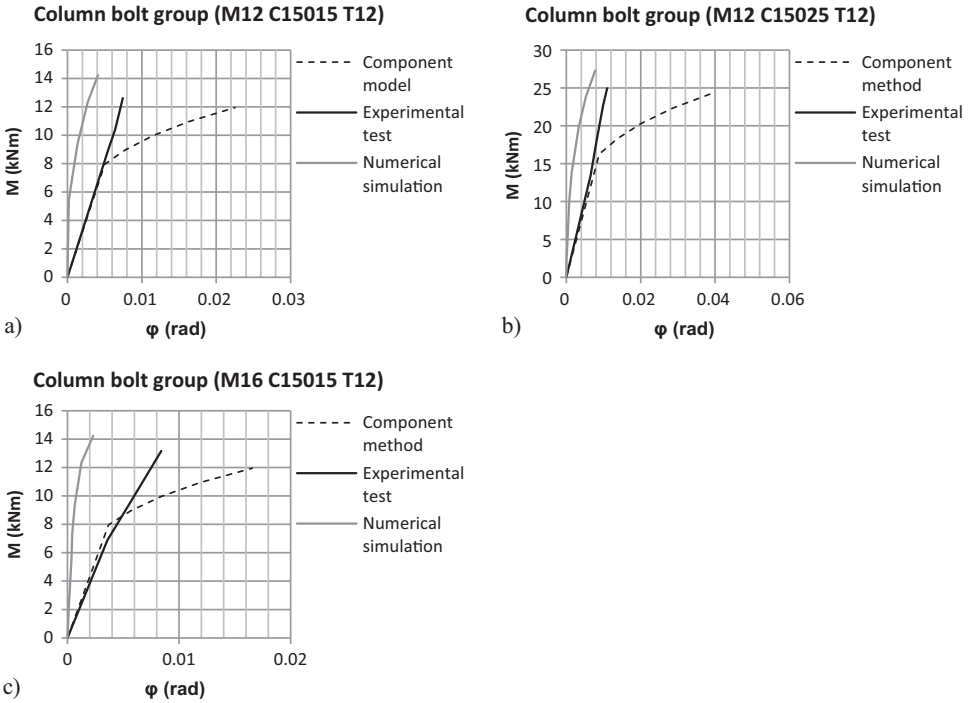

Fig. 12. $M - \varphi$ curves of the column bolt group of the specimens: (a) M12 C15015 T12; (b) M12 C15025 T12; (c) M16 C15015 T12.

shows a good agreement with both experimental test and numerical simulation results.

Fig. 14a, b, c gives the rotation of the joint resulting from calculations using the component method and numerical simulations for each specimen. From the results, it is seen that the proposed mechanical model using component method shows good agreement comparing with numerical simulation model, in terms of stiffness.

6. Conclusions

The analysis using the component method and experimental results on cold-formed steel beam-to-column bolted gusset-plate joints allow making the following conclusions:

The new "three-springs" mechanical model that integrates formulation proposed in this article and Eurocode3 rules for stiffness calculation of cold-formed steel beam-to-beam gusset plate joint was presented.

Analytical formula for the evaluation of T-form gusset plate stiffness calculation was derived. The stiffness calculated according to proposed method was compared with both laboratory test data and numerical simulations and showed good agreement.

The investigations showed that the stiffness coefficients that are

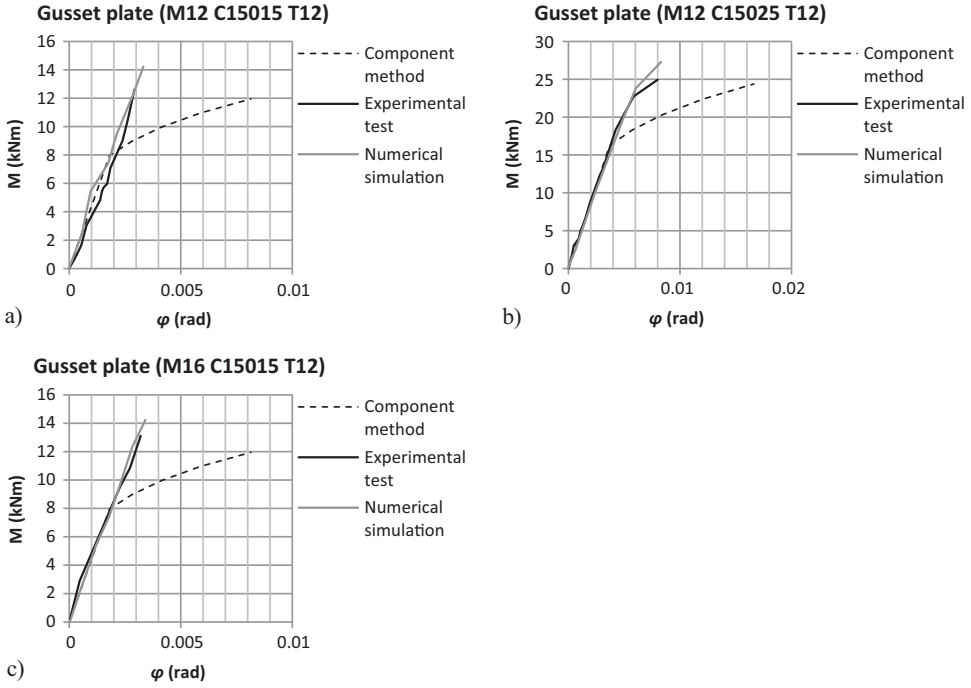

Fig. 13. $M - \varphi$ curves of the gusset plate of the specimens: (a) M12 C15015 T12; (b) M12 C15025 T12; (c) M16 C15015 T12.

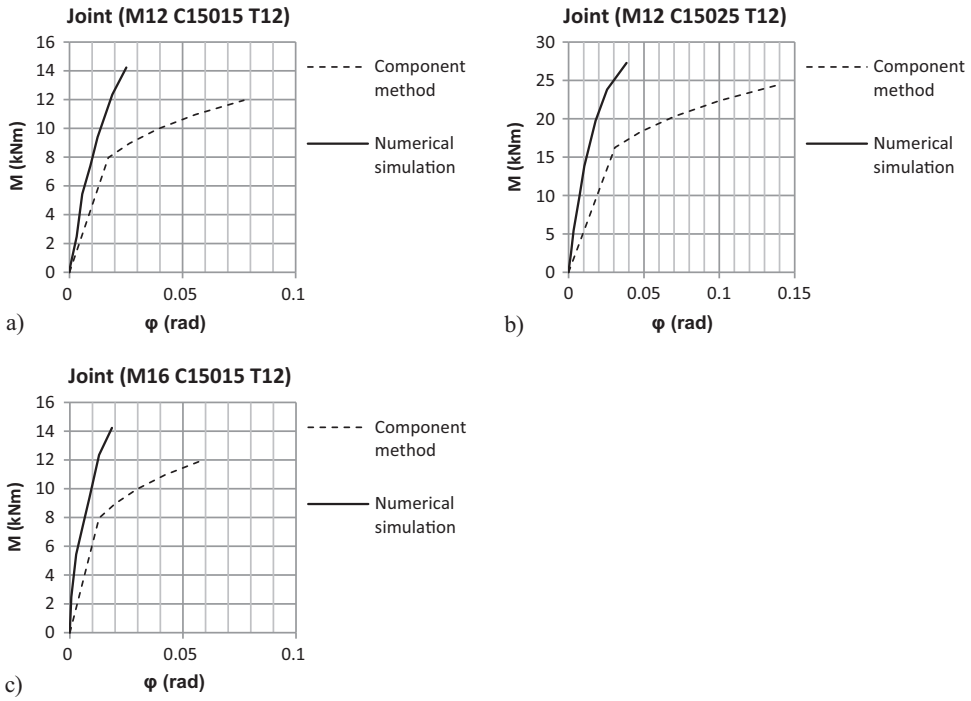

Fig. 14. $M - \varphi$ curves of joints: (a) M12 C15015 T12; (b) M12 C15025 T12; (c) M16 C15015 T12.

listed in Eurocode 3 part 1–8 (originally suitable for standard joints with elements that are 3 mm and thicker) could be applied to such cold-formed element joints.

References

[1] M. Braham, J.-P. Jaspart, Is it safe to design a building structure with simple joints, when they are known to exhibit a semi-rigid behaviour?, J. Constr. Steel Res. 60 (2004) 713–723.

[2] A.A. Del Savio, D.A. Nethercot, P.C.G.S. Vellasco, S.A.L. Andrade, L.F. Martha, Generalised component-based model for beam-to-column connections including axial versus moment interaction, J. Constr. Steel Res. 65 (8–9) (2009) 1876–1895.

[3] C. Diaz, P. Marti, M. Victoria, O.M. Querin, Review on the modelling of joint behaviour in steel frames, J. Constr. Steel Res. 67 (2011) 741–758.

[4] A. Daniūnas, K. Urbonas, Analysis of the steel frames with the semi-rigid beam-to-beam and beam-to-column knee joints under bending and axial forces, Eng. Struct. 30 (2008) 3114–3118.

[5] A. Daniūnas, K. Urbonas, Influence of the semi-rigid bolted steel joints on the frame behaviour, J. Civ. Eng. Manag. 16 (2) (2010) 237–241.

[6] A. Daniūnas, K. Urbonas, Influence of the column web panel behaviour on the characteristics of a beam-to-column joint, J. Civ. Eng. Manag. 19 (2) (2013) 318–324.

[7] G. Ćirović, V. Radonjanin, M. Trivunić, D. Nikolić, Optimization of UHPFRC beams subjected to bending using genetic algorithms, J. Civ. Eng. Manag. 20 (4) (2014) 527–536.

[8] M.M. Fayyadh, H.A. Razak, Analytical and experimental study on repair effectiveness of CFRP sheets for RC beams, J. Civ. Eng. Manag. 20 (1) (2014) 21–31.

[9] Z. Kala, Reliability analysis of the lateral torsional buckling resistance and the

ultimate limit state of steel beams with random imperfections, J. Civ. Eng. Manag. 21 (7) (2015) 902–911.
[10] I. Misiūnaitė, A. Daniūnas, A. Juozapaitis, Unconventional double-level structural system for underdeck cable-stayed bridges, J. Civ. Eng. Manag. 18 (3) (2012) 436–443.
[11] T. Talaslioglu, Optimization of geometrically nonlinear lattice girders. Part I: considering member strengths, J. Civ. Eng. Manag. 21 (4) (2015) 423–443.
[12] M. D'Aniello, E.M. Güneyisi, R. Landolfo, K. Mermerdaş, Analytical prediction of available rotation capacity of cold-formed rectangular and square hollow section beams, Thin-Walled Struct. 77 (2014) 141–152.
[13] H.C. Ho, K.F. Chung, Experimental investigation into the structural behaviour of lapped connections between cold-formed steel Z sections, Thin-Walled Struct. 42 (2004) 1013–1033.
[14] H.C. Ho, K.F. Chung, Analytical prediction on deformation characteristics of lapped connections between cold-formed steel Z sections, Thin-Walled Struct. 44 (2006) 115–130.
[15] H.C. Ho, K.F. Chung, Structural behavior of lapped cold-formed steel Z sections with generic bolted configurations, Thin-Walled Struct. 44 (2006) 466–480.
[16] K.F. Chung, H.C. Ho, Analysis and design of lapped connections between cold-formed steel Z sections, Thin-Walled Struct. 43 (2005) 1071–1090.
[17] K.F. Chung, H.C. Ho, A.J. Wang, An investigation into deformation characteristics of lapped connections between cold-formed steel z sections, Steel Struct. 5 (2005) 23–32.
[18] D. Dubina, V. Ungureanu, Behaviour of multi-span cold-formed Z-purlins with bolted lapped connections, Thin-Walled Struct. 48 (2010) 866–871.
[19] R. Gutierrez, A. Loureiro, M. Lopez, A. Moreno, Analysis of cold-formed purlins with slotted sleeve connections, Thin-Walled Struct. 49 (2011) 833–841.
[20] J. Yang, Q. Liu, Sleeve connections of cold-formed steel sigma purlins, Eng. Struct. 43 (2012) 245–258.
[21] Q. Liu, J. Yang, F. Wang, Numerical simulation of sleeve connections for cold formed steel sigma sections, Eng. Struct. 100 (2015) 686–695.
[22] R. Gutierrez, A. Loureiro, J.M. Reinosa, M. Lopez, Numerical study of purlin joints with sleeve connections, Thin-Walled Struct. 94 (2015) 214–224.
[23] J.B.P. Lim, D.A. Nethercot, Ultimate strength of bolted moment-connections between cold-formed steel members, Thin-Walled Struct. 41 (2003) 1019–1039.
[24] J.B.P. Lim, D.A. Nethercot, Stiffness prediction for bolted moment connections between cold-formed steel members, J. Constr. Steel Res. 60 (2004) 85–107.
[25] I. Elkersh, Experimental investigation of bolted cold formed steel frame apex connections under pure moment, Ain Shams Eng. J. 1 (2010) 11–20.
[26] P.M. Pernes, Z. Nagy, FE modeling of cold-formed steel bolted joints in pitch-roof portal frames, Acta Tech. Napoc.: Civ. Eng. Archit. 3 (2012) 234–242.
[27] F. Öztürk, S. Pul, Experimental and numerical study on a full scale apex connection of cold-formed steel portal frames, Thin-Walled Struct. 94 (2015) 79–88.
[28] M.F. Wong, K.F. Chung, Structural behaviour of bolted moment connections in cold-formed steel beam-column sub-frames, J. Constr. Steel Res. 58 (2002) 253–274.
[29] W.K. Yu, K.F. Chung, M.F. Wong, Analysis of bolted moment connections in cold – formed steel beam-column sub-frames, J. Constr. Steel Res. 61 (2005) 1332–1352.
[30] A.B. Sabbagh, M. Petkovski, K. Pilakoutas, R. Mirghaderi, Ductile moment – resisting frames using cold – formed steel sections: an analytical investigation, J. Constr. Steel Res. 67 (2011) 634–646.
[31] A.B. Sabbagh, M. Petkovski, K. Pilakoutas, R. Mirghaderi, Development of cold-formed steel elements for earthquake resistant moment frame buildings, Thin-Walled Struct. 53 (2012) 99–108.
[32] A.B. Sabbagh, M. Petkovski, K. Pilakoutas, R. Mirghaderi, Cyclic behaviour of bolted cold-formed steel moment connections: FE modelling including slip, J. Constr. Steel Res. 80 (2013) 100–108.
[33] Ž. Bučmys, G. Šaučiuvėnas, The behaviour of cold formed steel structure connections, Eng. Struct. Technol. 5 (3) (2013) 113–122.
[34] J.-P. Jaspart, General report: session on connections, J. Constr. Steel Res. 55 (2000) 69–89.
[35] J.-P. Jaspart, J.-P. Demonceau, European design recommendations for simple joints in steel structures, J. Constr. Steel Res. 64 (2008) 822–832.
[36] V.-L. Hoang, J.-F. Demonceau, J.-P. Jaspart, Resistance of through-plate component in beam-to-column joints with circular hollow columns, J. Constr. Steel Res. 92 (2014) 79–89.
[37] V.-L. Hoang, J.-P. Jaspart, J.-F. Demonceau, Hammer head beam solution for beam-to-column joints in seismic resistant building frames, J. Constr. Steel Res. 103 (2014) 49–60.
[38] V.-L. Hoang, J.-P. Jaspart, X.-H. Tran, J.-F. Demonceau, Elastic behaviour of bolted connection between cylindrical steel structure and concrete foundation, J. Constr. Steel Res. 115 (2015) 131–147.
[39] EN 1993-1-8: 2005. Eurocode 3 – Design of steel structures – Part 1–8: Design of joints, Comité Européen de Normalisation, Brussels, 2005.
[40] Ž. Bučmys, A. Daniūnas, Analytical and experimental investigation of cold-formed steel beam-to-column bolted gusset-plate joints, J. Civ. Eng. Manag. 21 (8) (2015) 1061–1069.
[41] L. Laim, J.P.C. Rodrigues, L.S. da Silva, Experimental and numerical analysis on the structural behaviour of cold-formed steel beams, Thin-Walled Struct. 72 (2013) 1–13.